

Type I Photosensitizers Based on Aggregation-Induced Emission

Subjects: [Materials Science](#), [Biomaterials](#)

Contributor: Danxia Li , Peiying Liu , Yonghong Tan , Zhijun Zhang , Miaomiao Kang , Dong Wang , Ben Zhong Tang

Photodynamic therapy (PDT) is emerging as a minimally invasive therapeutic modality with precise controllability and high spatiotemporal accuracy in the field of diseases treatment. PDT mainly relies on the photosensitizers (PSs) to generate oxidative reactive oxygen species (ROS), to play the therapeutic role. Type I photosensitizers, that undergo hydrogen atom abstraction or electron transfer manner and subsequently produce superoxide radical ($O_2^{\cdot-}$), hydroxyl radical (OH^{\cdot}), or hydrogen peroxide (H_2O_2), etc., is showing more and more prominent advantages, particularly in hypoxic tissues, since type I PSs-involved PDT usually exhibit distinctive hypoxia tolerance. Regarding the diverse type I PSs, aggregation-induced emission (AIE)-active type I PSs are currently arousing great research interest owing to their distinguished aggregation-induced emission and aggregation-induced generation of reactive oxygen species (AIE-ROS) features.

aggregation-induced emission

type I photosensitizers

phototheranostics

1. Introduction

Photodynamic therapy (PDT) was first defined in the middle of the 20th century when R. Lipson and S. Schwartz discovered the cancer diagnostic and therapeutic effects of a hematoporphyrin derivative (HpD) [1]. Since then, exploration in the field of PDT has continued without cessation [2,3]. Possessing the distinguished merits of non-invasiveness, high spatiotemporal precision, accurate controllability, and low systemic toxicity, PDT is currently captivating an unprecedented level of research interest as a pioneering and intriguing therapeutic modality, with significant advancements in PDT witnessed in the areas of cancer and various non-oncological disease therapies [4,5]. For example, the effectiveness of PDT in the treatment of skin, neck and superficial bladder cancers [6], as well as pathogen-[7,8] (e.g., propionibacterium acnes [9], human papilloma virus [10,11]) caused infectious diseases, has been experimentally or clinically validated.

Basically, PDT mainly relies on the oxidative reactive oxygen species (ROS), including singlet oxygen (1O_2), superoxide radical ($O_2^{\cdot-}$), hydroxyl radical (OH^{\cdot}), hydrogen peroxide (H_2O_2), etc., to play the therapeutic role, as ROS not only can cause direct killing of cancer cells or pathogens via destruction of the cellular components, but can also induce vascular damage as well as acute local and systemic immune response, to jointly eliminate tumors [12]. In the PDT process, ROS are generally produced via two types of photo-triggered reactions (namely, type I and type II) between the photosensitizers (PSs) and surrounding substrates [13]. To be specific, the type I reaction follows hydrogen atom abstraction or electron transfer manner, subsequently leading to the formation of radicals

and H₂O₂; alternatively, energy transfer from the electronically excited triplet-state PSs to the ground-state molecular oxygen is involved in the type II process accompanying ¹O₂ production [14]. In theory, these two competing photoreaction pathways can occur in parallel, but the type of PSs, oxygen concentration, as well as adjacent substrates, always cause one pathway to be dominant in the practical PDT process [15]. Owing to the relatively low excited energy required to form ¹O₂ from molecular oxygen, most of the reported PSs are inclined to undergo the oxygen-dependent type II PDT process, the therapeutic efficacy of which, however, is fatally impaired by the untoward predicament of the hypoxic microenvironments of the pathological tissues, such as the interior of a solid tumor or bacterial infection site [16,17]. By contrast, type I PDT has been proven to hold great potential in breaking through this inherent bottleneck, since diminished oxygen supply is required in a type I reaction [18].

The distinctive hypoxia tolerance and favorable therapeutic performance of type I PDT in hypoxic pathological tissues have largely spawned the evolution of type I PSs over the past several decades [19]. To date, profiting from the enormous efforts of people dedicated to the pursuit of puissant type I PDT, multifarious materials have been developed as type I PSs, including but not limited to metal oxides [20] (e.g., TiO₂), carbon-based nanomaterials [21,22] (e.g., carbon dots, *g*-C₃N₄), organic–inorganic hybrids [23,24] (e.g., metal–organic framework), transition metal complexes [25] (e.g., Ru(II) complexes), and organic molecules [26,27]. Unlike inorganic materials which suffer from poor biodegradability, complicated pharmacokinetics and worrisome biosecurity, organic molecules with their distinct advantages of favorable biocompatibility, satisfactory metabolism, facile processability, excellent reproducibility, structural diversity and easy tunability, stand out as a promising option for practical bioapplications [28,29]. In particular, some organic PSs are capable of enabling fluorescence imaging (FLI)-guided PDT due to their intrinsic fluorescence emission feature, which represents an important category of photo-driven theranostics [30,31,32].

The most eye-catching representatives are PSs with aggregation-induced emission (AIE) characteristics [33]. In addition to the common advantages of organic PSs, as a class of novel organic fluorophores, AIE PSs uniquely exhibit incomparable attributes of aggregation-induced emission and aggregation-induced generation of ROS (AIG-ROS), due to their twisted structures as well as their ornamentation with rich rotators or vibrators [34]. To be specific, AIE PSs usually show faint fluorescence emission and ROS generation in the dissolved state, because of the intramolecular motion-resulted excited energy consumption [35]. This nonradiative thermal dissipation, however, can be effectively suppressed upon aggregation due to the restriction of intramolecular motion (RIM), which consequently promotes fluorescence as well as the ROS generation-involved intersystem crossing (ISC) channel at the aggregate state [36]. In addition, the twisted conformation of AIE PSs can also significantly weaken the intermolecular π - π stacking after aggregation and, thus, ultimately contribute to AIE and AIG-ROS features [37]. Since most organic PSs are structurally hydrophobic and inevitably tend to form aggregates in aqueous physiological environments, by taking full advantage of aggregation, AIE PSs have earned a wider scope of application in the biomedical field, in contrast with traditional aggregation-caused quenching (ACQ) PSs, which usually suffer from diminished fluorescence emission and decreased ROS production at the aggregate state because of their rigidly planar conformations-caused competitive energy consumption [38].

2. Basic Principles of Type I PDT

In general, PSs, light source, and substrates, are recognized as three essential elements in PDT [4]. According to the Jablonski diagram shown in **Figure 1**, the PSs at ground singlet state (S_0) will, firstly, be excited to the unstable excited singlet state (S_1) upon light irradiation, and then return to their ground state via radiative or non-radiative decay in the manner of fluorescence emission or heat production. Notably, provided that the energy gap between S_1 and T_1 ($\Delta E_{S_1-T_1}$) is small enough, the excited singlet state PSs can preferably reach the relatively stable excited triplet-state (T_1) by undergoing the ISC process, in which state the PSs can survive long enough to carry out different photochemical reactions (including type I and type II) with surrounding substrates, to yield ROS [6]. Here, type I process will be emphasized.

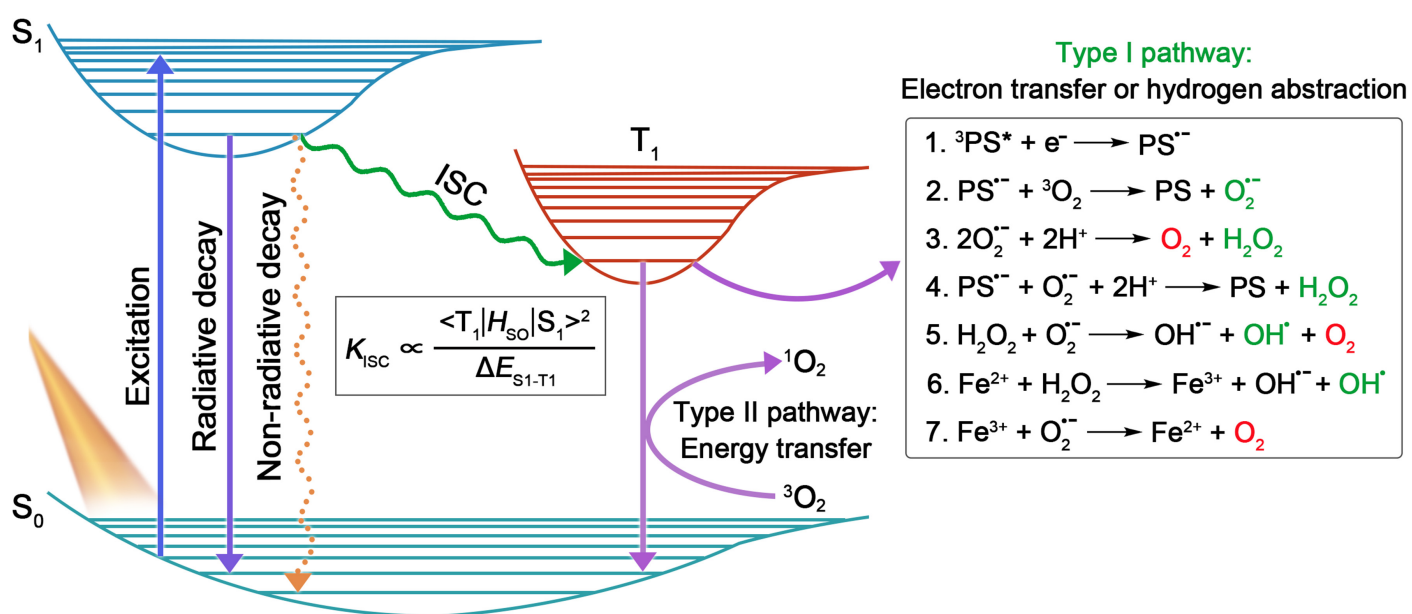


Figure 1. The illustration shows the working mechanisms of PSs described with the Jablonski diagram. The inserted box in the middle shows the ISC rate equation. The inserted box on the right shows the related cascaded reactions during the type I process.

Unlike the type II reaction involving a direct energy transfer to the triplet-state molecular oxygen to produce ${}^1\text{O}_2$, the type I process refers to the production of H_2O_2 and radicals (e.g., $\text{O}_2^{\bullet -}$, OH^{\bullet}) via several cascade electron transfer and hydrogen atom abstraction procedures [1]. Specifically speaking, the type I pathway usually begins with an initial one-electron reduction of the triplet-state PS (${}^3\text{PS}^*$) with the production of a PS radical anion ($\text{PS}^{\bullet -}$) (Reaction 1), which can further transfer one electron to molecular oxygen to produce $\text{O}_2^{\bullet -}$ (Reaction 2). By virtue of the disproportionation catalyzed by superoxide dismutase (SOD) (Reaction 3) or another one-electron reduction by $\text{PS}^{\bullet -}$ (Reaction 4), $\text{O}_2^{\bullet -}$ can be reduced to H_2O_2 . Then, the generated H_2O_2 can ultimately be transformed into highly oxidative OH^{\bullet} by reacting with $\text{O}_2^{\bullet -}$ or Fe^{2+} , known as the Haber–Weiss reaction (Reaction 5) and Fenton reaction (Reaction 6), respectively [41]. In this respect, the Fenton reaction can be augmented since the Fe^{3+} produced in this process can be reduced to Fe^{2+} by $\text{O}_2^{\bullet -}$ for recycling (Reaction 7) [42].

By making full utilization of the disproportionation reaction, Haber–Weiss reaction, or Fenton reaction, type I PDT has been proven to exhibit superior therapeutic outcomes in hypoxic environments, in contrast with type II PDT. This can be explained from the following aspects: (1) $O_2^{\bullet -}$ (few seconds) is recognized as having a much longer half-life than 1O_2 (10^{-5} s), which endows $O_2^{\bullet -}$ with a relatively long diffusion distance compared with others [43,44]; (2) featured with robust oxidative characteristic, OH^{\bullet} is the most biologically aggressive reactive oxygen centered radical that can cause direct damage to various vital biomacromolecules, thus, exerting amplified PDT response [45,46,47]; (3) unlike the heavy O_2 consumption of the type II pathway, the O_2 needed in the type I pathway can be recycled among its reactions, which can enable the limited O_2 in hypoxic conditions to be fully utilized, and endow type I PDT with good hypoxia tolerance [18].

3. Applications of Type I AIE PSs

On the basis of the mechanism described above, type I PSs exhibit relatively low external O_2 requirements, owing to the recyclable O_2 utilization in the type I ROS generation process. Intrinsically, type I AIE PSs enable the crafty integration of aggregation-induced fluorescence emission and enhanced ROS generation with minimized O_2 dependence, presenting significant theranostic potential in different biomedical applications, including, but not limited to cancer ablation, bacterial infection elimination, and harmful algal bloom suppression.

3.1. The Anti-Tumor Applications

Due to the aggressive proliferation of cancer cells and insufficient blood supply, hypoxia often takes place in the microenvironments of solid tumors, thus, severely hindering the generation of type II ROS as it is highly dependent on ambient O_2 concentration. Conversely, type I PDT has manifested great potential in ablating hypoxic tumors, profiting from its lower O_2 demand nature. Based on this, AIE PSs featuring type I ROS-generating properties will be ideal candidates for potent PDT, with superb therapeutic outcomes.

For the purpose of redshifted absorption and emission wavelengths, as well as boosted theranostic performance, AIE PSs and other organic PSs are generally engineered to contain multiple aromatic rings and/or large conjugated units in their molecular structures, giving rise to their high hydrophobicity. In order to facilitate the in vivo biological applications, hydrophobic AIE PSs are commonly encapsulated within nanovehicles based on amphiphilic biocompatible matrices to form well-dispersed AIE nanoparticles (NPs) in aqueous physiological environments [48]. Additionally, bright fluorescence, excellent ROS production and enhanced permeability and retention (EPR) effect-driven tumor location can be successfully achieved, simultaneously, after nanofabrication, since the aggregation of AIE PSs within the intraparticle limited room is capable of effectively restricting their active intramolecular motions, thus, blocking nonradiative thermal dissipation and saving the excited state energy for the fluorescence and ISC pathway [28,31]. In addition to passively targeted tumor enrichment by the EPR effect, actively targeting transport of AIE PSs favored by specific recognition will be able to further enhance PDT efficacy. From those, Lou et al. [49] developed an amphiphilic polymeric matrix with conjugated targeting peptides to co-assemble with a type I AIE PS of TTB to fabricate tumor-specific targeting TTB NPs for amplifying type I photodynamic cancer treatment. In addition, Duo et al. [50] put forward an innovative protocol for efficiently targeted delivery of type I AIE PSs to tumor

tissues by taking full advantage of the hypoxia condition in solid tumors and selective hypoxia tropism of some bacteria. For this approach, a novel bacteria-based AIE hybrid system was built, enabling the powerful delivery of type I AIE PS of TBP-2 into the hypoxic tumor microenvironments for hypoxia-tolerant PDT of orthotopic colon cancer.

Considering that the effective killing range of ROS is typically confined to the immediate vicinity of PSs on a subcellular scale, an appropriate organelle-targeting location of PSs is, therefore, highly desired for implementing final PDT outcomes. Different subcellular organelles play their own unique roles in maintaining the normal physiological function of cells. It has been acknowledged that the organelles, including cell membrane, mitochondria, lysosomes, ER, and nucleus, are all valid sites for performing PDT [51]. To date, diverse subcellular organelle-targeted type I AIE PSs-based anti-tumor systems have been exploited in succession [52]. For instance, Feng et al. [53] developed a class of cationic AIE PSs possessing a specific tumor cell mitochondrial targeting feature to facilitate both type I and type II PDT. In addition, Tang et al. [54] proposed a useful molecular design guideline for constructing efficient AIE PSs and tailoring their organelle specificity.

Among the various subcellular organelles, of particular importance is the cell nucleus as it dominates the cellular gene expression, metabolism and proliferation [55]. Moreover, the DNA and RNA parts of the nuclei are very sensitive to type I ROS due to its extremely high chemical reactivity [56]. In view of this, Wang et al. [56] explored, for the first time, a nucleus-targeting PDT strategy based on type I AIE PSs, by making full use of theranostic agents and nanocarrier systems (**Figure 2a**). Two AIE PSs, named TFMN and TTFMN, with typical D–A structures and sufficient molecular rotors, were firstly designed and synthesized. Compared with TFMN, TTFMN was equipped with additional TPE moiety in structure, which endowed it with much better AIE peculiarity. Various ROS indicators were employed to distinguish the ROS species produced by TFMN and TTFMN, through fluorescence spectroscopy and ESR measurements, which was discriminated to type I ROS of OH[•]. Moreover, the TTFMN showed stronger ESR signal intensity than TFMN (**Figure 2b**), indicating its better generation capacity of OH[•], which was attributed to its superior AIE tendency and smaller $\Delta E_{S_1-T_1}$. With the help of a lysosomal acid-activated nuclear localization signal peptide (TAT)-modified amphiphilic polymer, the resultant TTFMN-loaded NPs (TTFMN-NPs) exhibited nucleus-anchoring delivery ability, visualized by the intrinsic fluorescence property of TTFMN (**Figure 2c**). Further in vivo investigations uncovered that TTFMN-NPs with good biosecurity and long blood circulation time could specifically accumulate at tumor sites (**Figure 2d**). Upon white light irradiation, TTFMN-NPs induced high-efficiency tumoricidal results with a 75.1% tumor growth inhibition rate (**Figure 2e,f**). This work offered a new perspective in the construction of type I PS-based and nucleus-targeted nanotheranostic systems.

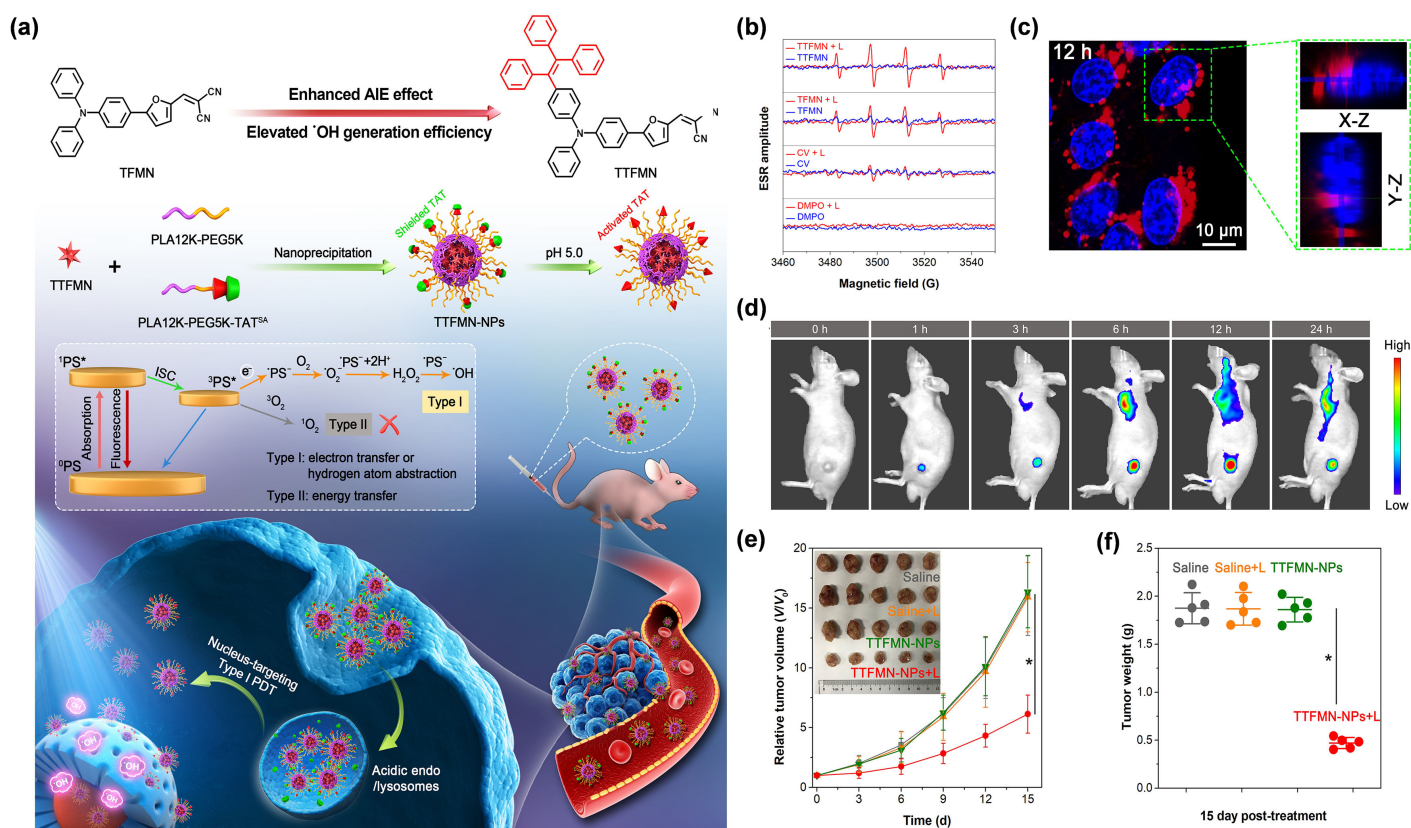


Figure 2. (a) Illustration of molecular design principle, nanotheranostics fabrication, and its application in nucleus-targeted type I photodynamic cancer treatment. (b) ESR analysis for OH^\bullet generation of TTFMN and TFMN after white light irradiation (200 mW/cm^2). (c) CLSM images of nuclear targeting delivery of TTFMN-NPs ($2 \mu\text{g/mL}$ TTFMN) after incubation with 4T1 cells for 12 h. The blue color represents the fluorescence of Hoechst 33342 for locating cell nucleus and the red color represents the fluorescence of TTFMN-NPs. (d) Time-dependent in vivo FLI of tumor-bearing mice after injection with TTFMN-NPs. (e) The growth curves of tumors in different treatment groups ($n = 5$, $*p < 0.001$). (f) The tumor weights of mice after treatments for 15 days ($n = 5$, $*p < 0.001$). Reprinted with permission from [56], copyright 2021, Wiley-VCH.

At present, most AIE PSs can only be effectively excited by short wavelength of UV or visible lights. However, the shallow penetration depth of the excited light presented a major scientific challenge for AIE PSs to treat deep-seated tumors. Based on this, the combination of rare earth doped upconversion NPs (UCNPs) would provide an effective solution to this problem, since UCNPs can serve as a near-infrared (NIR) light transducer to harness and convert the NIR laser to UV-visible light, enabling the construction of robust NIR laser excitable nanotheranostic systems [57]. Encouraged by the synergistic effect of combining UCNPs and AIE PSs toward cancer therapy, Wang et al. [58] creatively designed and developed a triple-jump photodynamic nanotheranostic agent, termed MUM NPs, by integrating a type I AIE PS of MeOTTI into the multifunctional nanoplatform built by UCNPs and manganese dioxide (MnO_2), for enhanced theranostic outputs in PDT (Figure 3a). Specifically, MeOTTI was engineered to afford the type I ROS capacity verified by the ESR test (Figure 3b). With the aid of UCNPs whose emission spectrum matched well with the absorption spectrum of MeOTTI, the resulting Förster resonance energy transfer (FRET) effect between UCNPs and MeOTTI not only achieved the excitation light extension from UV-

visible to NIR region, but also significantly elevated the ROS generation efficiency (**Figure 3c**). Attractively, the introduction of the MnO_2 component was aimed at depleting the intracellularly upregulated glutathione (GSH), thus, significantly facilitating the production of highly oxidative type I ROS in cells. Meanwhile, the yielded Mn^{2+} was also able to catalyze the intracellular H_2O_2 to generate OH^{\bullet} , as well as for magnetic resonance imaging (MRI). Therefore, the triple-jump type I ROS generation of MUM NPs could be smoothly achieved inside the tumor cells after NIR laser irradiation. This splendid triple-jump photodynamic theranostic protocol was confirmed by a series of cell and animal experiments (**Figure 3d,e**).

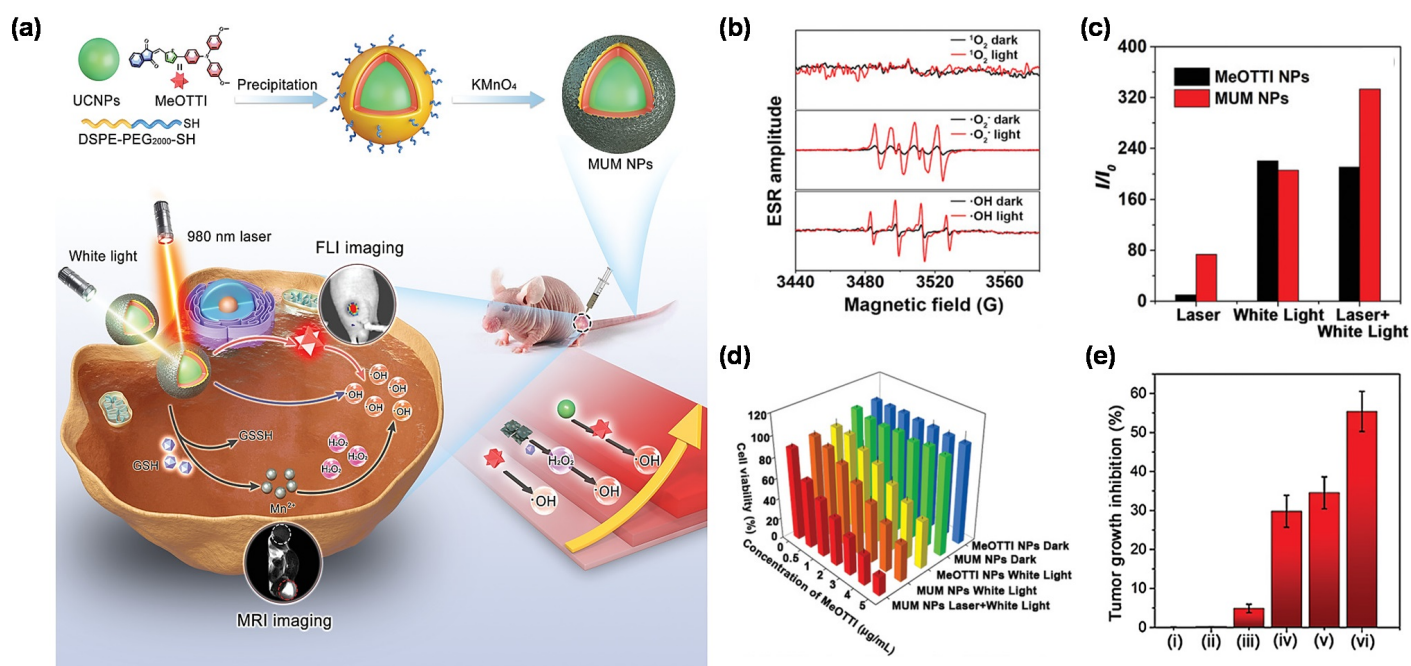


Figure 3. (a) Chemical structure of MeOTTI and schematic illustration of triple-jump photodynamic theranostic protocol. (b) ROS generation type of MeOTTI determined by ESR test. (c) ROS production efficiency of MeOTTI NPs and MUM NPs at the same MeOTTI concentration under the irradiation of different light sources. (d) Cell viability of 4T1 cells treated with different conditions. (e) Tumor inhibition ratios of mice after different treatments, namely: (i) PBS, (ii) MUM NPs, (iii) 980 nm laser and white light, (iv) MeOTTI NPs and white light, (v) MUM NPs and white light, (vi) MUM NPs, 980 nm laser and white light ($n = 5$, $* p < 0.001$). Reprinted with permission from [58], copyright 2021, Wiley-VCH.

In addition to being assisted by UCNPs, exploring AIE PSs with an outstanding two-photon absorption property was another effective method to break through the obstacles encountered by short-wavelength excitation [59]. Moreover, AIE PSs have proved to be promising candidates for developing two-photon excitable PDT agents, as the two-photon absorption cross section ($\delta_{2\text{PA}}$) of AIE PSs could obviously be raised by simply increasing their loading amount in the NPs, exhibiting a unique aggregation-enhanced nonlinear optical effect [60]. Generally, the wavelength in two-photon excitation is twice as long as that of one-photon absorption, thus, making the NIR light-excitable photodynamic theranostics feasible. In this regard, Tang et al. [61] constructed amphiphilic lipids-enveloping AIE NPs by encapsulating a tactfully designed two-photon excitable type I AIE PS (TPE-PTB) (**Figure**

Infectious diseases caused by pathogenic microbes including bacteria, fungi, and viruses, pose serious threats to humans, since they usually cause severe diseases such as foodborne illness, tuberculosis, sepsis, meningitis, and pneumonia, for which the situation continues to worsen, along with the appearance of antibiotics-resistant microbes [62,63]. In view of this rigorous challenge, PDT has stood out as a promising candidate for antimicrobial applications including the inactivation of multidrug resistant (MDR) microbe species; ROS could provide an aggressive attack on microbes without the need for complete entrance of PSs into the microbial interior, which can potentially avoid the generation of microbial resistance [64]. In this respect, type I PDT has been widely employed due to the longer half-life of $O_2^{\cdot-}$, as well as the strong oxidizing property of OH^{\cdot} . Possessing the advantage of AIE and AIG-ROS, periodical achievements in the FLI-guided PDT of pathogenic microbes have been attained, based on AIE-active type I PSs [65,66,67].

For example, Wang et al. [68] reprepared a functional nanofibrous membrane (TTVB@NM) by doping a type I AIE PSs TTVB in an electroactive polymer (PVDF-HFP) matrix using the electrospinning technique, and achieved the photodynamic elimination of pathogenic droplets and aerosols under sunlight (**Figure 5a**). Due to the inherent positive charge, TTVB was able to effectively stain several kinds of bacteria and fungi (**Figure 5b**). Under sunlight irradiation, TTVB possessed outstanding type I ROS generation efficiency (**Figure 5c–e**), owing to its typical D–A structure and electron-rich heteroatoms (S and N). After doping into the PVDF-HFP, the obtained nanofibrous membrane (TTVB@NM) was demonstrated to exhibit similar photophysical performances as TTVB, as well as favorable washability and photostability, indicating great potential for effective antimicrobial effect. The antimicrobial activity of TTVB@NM was subsequently verified by the significantly decreased survival rates of four kinds of pathogenic droplets (Gram-positive bacteria *S. aureus*, Gram-negative bacteria *E. coli*, fungi *C. albicans*, and M13 bacteriophage) after 1 h under sunlight irradiation (**Figure 5f**). Further evaluation of the antimicrobial effect of TTVB@NM against pathogenic aerosols was carried out by placing the pathogenic aerosols-loaded TTVB@NM outdoors (**Figure 5g**). The results revealed that TTVB@NM could effectively inactivate pathogenic aerosols containing bacteria (inhibition rate: > 99%), fungi (~88%), and viruses (>99%) within only 10 min under sunlight irradiation (**Figure 5h,i**). The author also stated that TTVB was measured to show moderate photothermal conversion performance, which could play an adjuvant role for microbe inhibition.

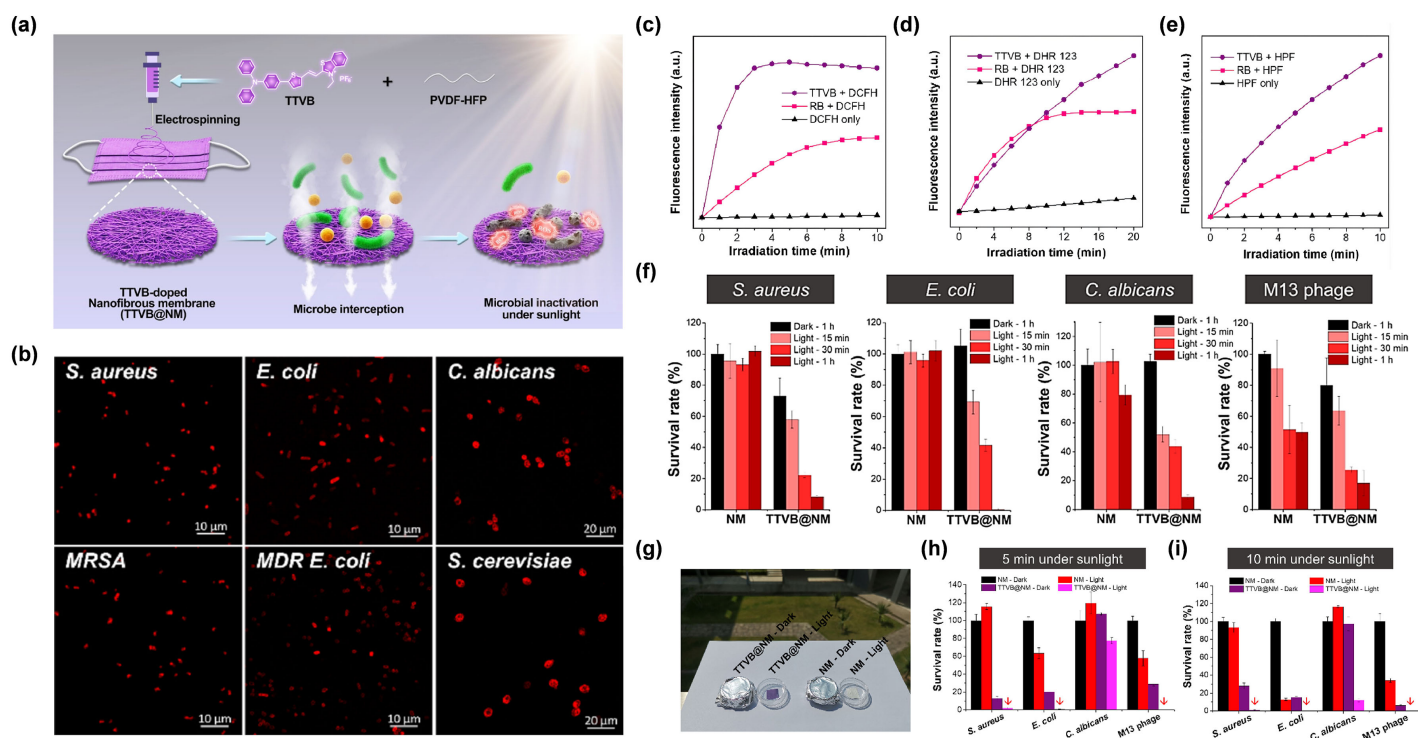


Figure 5. (a) Diagram of the preparation of TTVB@NM for antimicrobial applications. (b) CLSM imaging of bacteria and fungi co-incubated with TTVB. Relative fluorescence intensity of (c) DCFH for total ROS detection, (d) DHR123 for $O_2^{\cdot-}$ detection, and (e) HPF for OH^{\cdot} detection of TTVB and RB under light irradiation (34 mW/cm^2). (f) Microbial survival rate treated with NM or TTVB@NM in dark or under sunlight irradiation. (g) Antimicrobial experiment against pathogenic aerosols in dark or under sunlight irradiation. Survival rate of microbes under sunlight irradiation for (h) 5 min and (i) 10 min. Reprinted with permission from [68], copyright 2021, Elsevier.

3.3. The Inhibition of Harmful Algal Bloom

Harmful algal bloom (HAB) has become a global environmental problem, causing serious impact on aquatic ecology and economy [69]. The rapid growth of algae aggravates O_2 depletion and the release of harmful toxins, consequently threatening the survival of aquatic animals, resulting in widespread freshwater and marine area pollution [70]. Although many physical and chemical methods have been developed to inhibit HAB, their inherent drawbacks, such as low suppression rate, limited application area, and the possibility of secondary and persistent pollution, have hindered their widespread application [71]. In recent years, ROS-generating algacides have aroused extensive interest owing to their effective, eco-friendly and cost-efficient properties [72]. Therefore, exploring PSs which show excellent elimination effect of algae upon light irradiation without causing toxicity to other aquatic organisms, will be a promising strategy. Of particular interest are the type I AIE PSs, which can exhibit excellent ROS generation ability under low O_2 concentration, suitable for the relatively low O_2 environment of algal bloom.

Under this circumstance, Luo et al. [73] developed a water-soluble type I AIE PS with self-degrading ability, termed TVP-A, which could selectively eliminate HAB upon exposure to natural light (Figure 6a). TVP-A was constructed with a typical D–A structure with a primary amino group modified onto the terminal pyridinium, endowing the

molecule with good water solubility. Moreover, the positively charged property also endowed TVP-A with a specific algae-targeting feature, on account of the negatively charged cell membrane of the algae. Upon white light irradiation, TVP-A exhibited superb ROS generation ability through both type I and type II mechanisms, particularly $\cdot\text{OH}$. In this work, they co-incubated one cyanobacteria (*M. aeruginosa*) and two freshwater green algae (*C. vulgaris*, and *C. reinhardtii*) with TVP-A at different concentrations, respectively, under 16 h light ($50 \mu\text{Einstein}/\text{m}^2/\text{s}^1$)/8 h dark cycles to explore the effective concentrations in controlling the HAB. It was found that the 50% effective concentration (EC_{50}) value of TVP-A was less than 1 ppm for these three kinds of algae (**Figure 6b**). As shown in **Figure 6c**, in contrast with the commercial algaecide (Alg), which still had a large amount of algae residue when the concentration was as high as 100 ppm, TVP-A exhibited ultra-efficient control of HAB, with effective inhibition of the algae bloom *C. reinhardtii* at 5 ppm and a clear color of water after five natural daily cycles at 10 ppm. The fluorescence change of chlorophyll in *C. reinhardtii* was measured to prove the irreversible damage of chloroplast due to the photodynamic process (**Figure 6d**). After 2 h of illumination, the fluorescence intensity of chlorophyll decreased to less than 20%, indicating that TVP-A could rapidly cause irreversible damage to these important organelles of algal cells, at especially low concentration, upon illumination. Collectively, TVP-A could be employed as a powerful agent for inhibiting HAB by destroying the chloroplast of algal cells. In addition, the strong self-degradation ability of TVP-A (**Figure 6e**) suggested that it was an eco-friendly agent with little environmental residue left under sufficient natural light irradiation, avoiding secondary pollution to the environment. Meanwhile, the daily heart rates of fish in the groups with or without TVP-A showed no significant difference (**Figure 6f**), generally indicating the good biocompatibility of TVP-A within the working concentration. This strategy afforded a favorable insight into developing novel type I ROS-generating algaecides for green HAB governance.

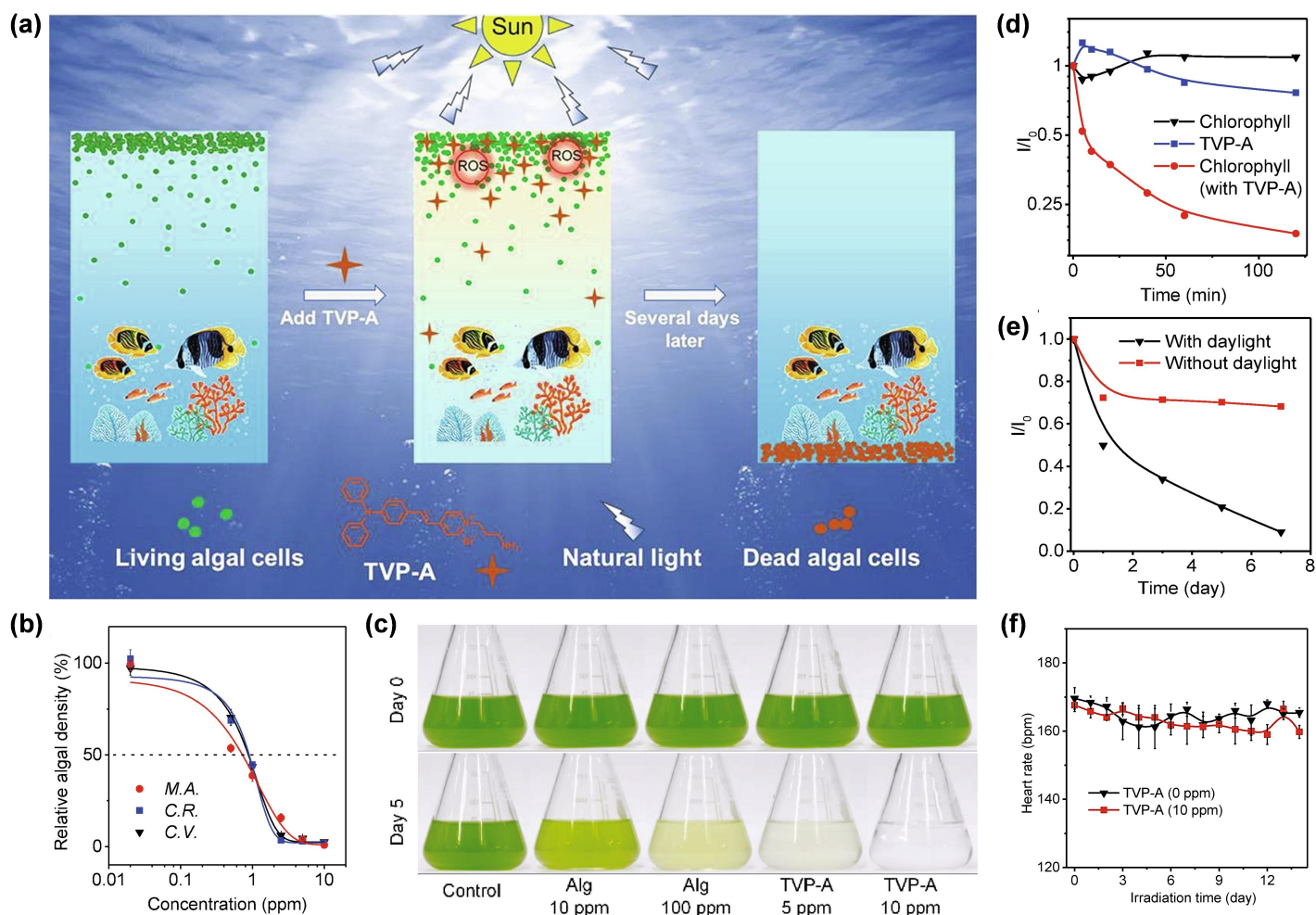


Figure 6. (a) Schematic illustration of selectively removing HAB by TVP-A upon natural light irradiation. (b) Relative cell density of three algae after incubating with TVP-A at different concentrations after 96 h under the simulated daily cycles. M.A.: *M. aeruginosa*; C.R.: *C. reinhardtii*; C.V.: *C. vulgaris*. (c) Photos of *C. reinhardtii* (1.6 × 10⁷ cells/mL) in the presence of Alg (10 ppm and 100 ppm) or TVP-A (5 ppm and 10 ppm) under the simulated daily cycles on day 0 and day 5. (d) The change of the relative fluorescence intensity (I/I_0) in *C. reinhardtii* (1.6 × 10⁷ cells/mL) in the presence or absence of TVP-A (5 ppm) under different times of simulated natural light illumination. (e) Variation in relative absorbance of TVP-A at 462 nm with or without different natural light for evaluating the degradability of TVP-A. (f) The change of average heart rates of fish with or without TVP-A during the 14 days of cultivation time under the simulated daily cycles. Reprinted with permission from [73], copyright 2021, Elsevier.

Retrieved from <https://encyclopedia.pub/entry/history/show/66537>